Chemical Science

ROYAL SOCIETY OF CHEMISTRY

EDGE ARTICLE

View Article Online
View Journal | View Issue

Cite this: *Chem. Sci.*, 2023, **14**, 1479

All publication charges for this article have been paid for by the Royal Society of Chemistry

Doping of charge-transfer molecules in cocrystals for the design of materials with novel piezo-activated luminescence†

Xiu Yin,[a] Chunguang Zhai,[a] Shuhe Hu,[a] Lei Yue,[a] Tongge Xu,[a] Zhen Yao,[a] Quanjun Li,[a] Ran Liu,[a] Mingguang Yao,*[a] Bertil Sundqvist[b] and Bingbing Liu[a]

Received 16th November 2022
Accepted 11th January 2023

DOI: 10.1039/d2sc06315h

rsc.li/chemical-science

A novel piezo-activated luminescent material with wide range modulation of the luminescence wavelength and a giant intensity enhancement upon compression was prepared using a strategy of molecular doping. The doping of THT molecules into TCNB-perylene cocrystals results in the formation of a weak but pressure-enhanced emission center in the material at ambient pressure. Upon compression, the emissive band from the undoped component TCNB-perylene undergoes a normal red shift and emission quenching, while the weak emission center shows an anomalous blue shift from 615 nm to 574 nm and a giant luminescence enhancement up to 16 GPa. Further theoretical calculations show that doping by THT could modify intermolecular interactions, promote molecular deformation, and importantly, inject electrons into the host TCNB-perylene upon compression, which contributes to the novel piezochromic luminescence behavior. Based on this finding, we further propose a universal approach to design and regulate the piezo-activated luminescence of materials by using other similar dopants.

Introduction

The responses of luminescent materials to external stimuli, such as pressing, shearing and stretching, determine their potential for practical applications, such as pressure sensors, optical data storage and optoelectronic devices.[1–9] The design of piezoluminescent materials with desired properties is thus important to satisfy the requirements of different applications.[10–12] As one of the most common stimuli, pressure has been used to study the responses of luminescent materials upon compression.[13–16] In particular, organic molecular crystals with weak intermolecular interactions, such as van der Waals forces, hydrogen bonding, charge transfer, *etc.*, have been attracting intensive research interest in this field, in which π-conjugated molecules are commonly used as building blocks due to their unique optical and electronic properties combined with their high sensitivity to the environment.[17–19] According to the tight binding model, compression induced strengthening of intermolecular interactions could widen energy bands and thus reduce the energy gap,[20] while the enhanced interactions such as π–π interaction, could also lead to emission quenching.[21] Therefore, most luminescent materials known so far show a gradually red-shifted and quenched emission upon compression.[4,22–25] The design of piezochromic luminescent materials with anomalous compression responses for specific applications has long been pursued but remains a challenging task.

To date, piezochromic luminescence with anomalous blue-shifted and enhanced emission upon compression has been rarely reported. Three recent studies reported the observation of such piezochromic luminescence behaviors upon compression, either by designing a synthetic molecule with complicated compositions[17,26] or a ternary cocrystal in which the inert molecules play roles in controlling the intermolecular interactions of the donor–acceptor.[27] However, restricted by the compression-enhanced intermolecular interactions, the amount of blue shift and/or magnitude of luminescence enhancement remain limited and a universal mechanism to design such piezochromic luminescent materials remains lacking. Unlike these studies, doping of materials could change their electronic structure, causing impurity energy levels, lattice defects, stress strains, *etc.*, affect the luminescent properties of materials,[28] and thus provide a new way for luminescent material design.[29,30] Doping of organic molecular crystals has been recently reported to tune luminescence properties (including the lifetime and light emitting region) of photoluminescent materials under ambient conditions,[31,32] but the design of piezochromic luminescent materials by the doping strategy remains unexplored.

Here, we report that doping of tetrahydrothiophene (THT) into perylene-1,2,4,5-tetracyanobenzene (TCNB) cocrystals (PTCs) leads to the formation of a new weak emission center in the material, together with the strong emission band of the host binary cocrystal at ambient pressure. Surprisingly, this weak emission exhibits an

[a]State Key Laboratory of Superhard Materials, College of Physics, Jilin University, China. E-mail: yaomg@jlu.edu.cn

[b]Department of Physics, Umeå University, Sweden

† Electronic supplementary information (ESI) available. See DOI: https://doi.org/10.1039/d2sc06315h

anomalous pressure-enhanced luminescence response, resulting in a novel piezo-activated luminescence with a wide range of emission wavelength modulation and giant intensity enhancement in the material, exceeding that of previously reported materials. Further theoretical simulations give a new insight into the novel piezochromic luminescence responses in the doped cocrystals. This doping strategy is universal and can be extended to other analogous dopants for luminescence regulation and thus provides a new way for designing desirable piezo-activated materials with a tunable magnitude and pressure range.

Results and discussion

The perylene-TCNB cocrystals (PTCs) are synthesized by a typical solvent evaporation method[33] and emit strong visible luminescence under ambient conditions.[27] For the doping experiments, we soaked the PTCs in a THT liquid solution in a DAC, leading to the formation of THT doped PTCs (PTCs:THT). The successful doping of PTCs has been further confirmed by our energy dispersive spectrometry (EDS) measurements on the samples, which clearly shows the distribution of element S from the THT dopant in the crystals (Fig. S1†). To characterize the THT doped PTCs, we performed synchrotron XRD measurement on the sample in a DAC. The recorded XRD pattern is different from that of the PTCs without THT doping (Fig. S2(a)†), and can be well-indexed by a triclinic structure and the structure was refined by using the Rietveld method (Fig. 1(a)). The unit cell parameters can be given further as $a = 7.6875$ Å, $b = 29.1350$ Å and $c = 8.6946$ Å. Based on this, the molecular packing in the PTCs:THT crystals is demonstrated in Fig. S2(b),† that is, TCNB and perylene are alternately arranged to form a molecular column (-DADA-), which are closely packed in the surroundings, while the doped THT forms a trace of "ternary clusters" with TCNB and perylene (PTC-THT) in the crystals. In this case, the intercalated THT molecules pull TCNB towards the central axis of perylene, and the π–π overlap between one TCNB molecule and the adjacent perylene molecules is about half of a perylene plane. With these structural features, the luminescence spectra of PTCs:THT show a strong emission band (P1) at 728 nm and a new weak emission center (P2) at ~600 nm at ambient pressure (Fig. S3(a)†). This is different from the luminescence spectra of undoped PTCs, which only shows one emission peak at 712 nm. Note that the P2 should be from the ternary cluster PTC-THT in the crystals, which acts as a new emission center and will be discussed below.

High pressure was further used to tune the intermolecular interactions in the THT doped PTCs. Remarkably, the doped cocrystals exhibit a novel luminescence behavior as the pressure increases, as shown in Fig. 1(b). P1 exhibits a red shift and an

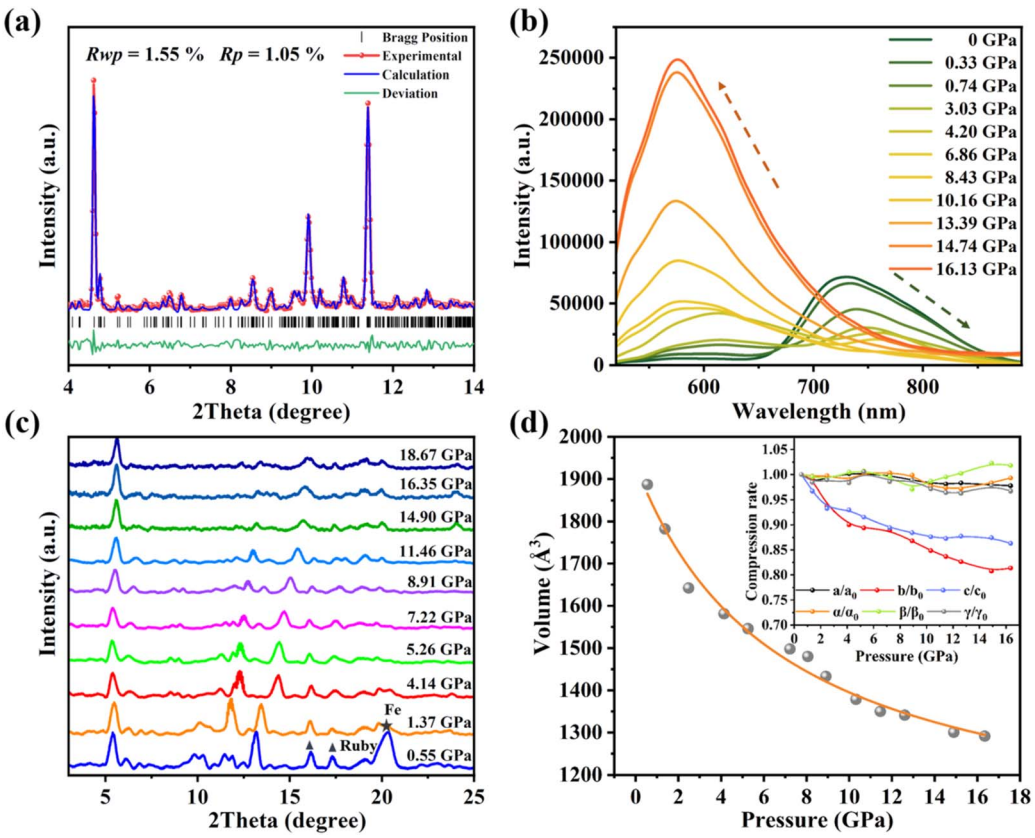

Fig. 1 (a) Synchrotron XRD pattern of PTCs:THT at 0.53 GPa. Rietveld refinement is used to fit the XRD pattern with $R_{wp} = 1.55\%$ and $R_p = 1.05\%$; (b) high-pressure luminescence spectra of PTCs:THT; (c) high-pressure XRD patterns of PTCs:THT; (d) plotted curves for the unit cell volume of PTCs:THT as a function of pressure. The inset shows the compression rate of lattice constants as the pressure increases. The XRD patterns are analyzed by JADE.

emission quenching up to 4.20 GPa, which is consistent with our observation of the luminescence response of binary cocrystal PTCs upon compression. In contrast, P2 shows an anomalous blue shift in the emission wavelength and a gradual intensity enhancement upon compression. Note that the luminescence intensity is 45 times higher than the initial intensity at a pressure of 16.13 GPa, which is also the highest pressure at which the luminescence intensity still increases in any piezochromic luminescent materials reported up to now. As the pressure increases further, a continuous red shift and emission decrease were observed at above 16.13 GPa (Fig. S3(b)†). The spectral coordinates show that the emission color changes from red to orange-yellow during compression (Fig. S3(c)†). It is clear that doping of the cocrystal changes its optical properties remarkably.

To further understand the novel luminescence response of the THT doped PTCs upon compression, we performed high pressure XRD measurements on the sample and the results are shown in Fig. 1(c). All representative diffraction peaks are upshifted to larger angles during compression and no new peak appeared. We further calculated the unit cell volume of the doped PTCs at various pressures and the curve for the unit cell volume as a function of pressure is shown in Fig. 1(d). These results suggest that the crystal lattice is progressively compressed and that no structural transition occurs. Note that the *a*-, *b*- and *c*-axes exhibit different pressure evolutions upon compression, indicating an anisotropic compression of the lattice. Furthermore, the *a*- and *b*-axes were more compressible than the *c*-axis, indicating that the distance between perylene and TCNB is reduced in the binary component, while the interaction between THT and perylene-TCNB is effectively enhanced due to the reduced space at the dopant sites. This should be related to the anomalous luminescence response of the THT doped PTCs upon compression.

In order to understand the anomalous phenomena observed in the experiments, we performed a detailed theoretical simulation. Note that, in our previous studies, the binary PTC cocrystals exhibit a normal emission red shift and quenching upon compression in both the experiment and theory.[27] In contrast, the anomalous luminescence response in PTCs:THT should be caused by the dopant effect of the ternary components in the cocrystals. We thus calculated the luminescence properties of THT doped PTC by a quantum mechanics and molecular mechanics (QM/MM)[34,35] method and focused on the properties of the ternary compound (PTC-THT). An approximate model has been used for our simulation (Fig. S4(a) and (b)†), in which the centers of the three components are in the same vertical plane and the donor–acceptor molecules are arranged alternately. Such a stacked structure is the same as that in our experiment and should give a very reasonable description of our THT doped PTC system. The luminescence spectra, emission wavelength and oscillator strength of PTC-THT at high pressure have been calculated and the results are shown in Fig. 2. According to our calculation, a significant luminescence intensity enhancement and emission blue shift can be clearly seen with increasing pressure, which agrees well with our experimental observations. In particular, PTC-THT exhibits a 54 times luminescence enhancement (oscillator strength increases from $f = 0.0047$ to $f = 0.2560$) and a large blue shift in the emission wavelength from ambient pressure to 22 GPa.

As we know, the oscillator strength is proportional to the overlap of the orbit,[36] and this overlap is strongly affected by the intermolecular interactions and the molecular configuration. Our simulations of the intermolecular interactions of the PTC-THT system upon compression demonstrate that, besides a routine increase in the steric interaction, the π–π stacking interaction becomes weaker compared with that of the undoped PTCs due to the fact that the doped THT molecules force the TCNB to move to the edge of the perylene molecules, and a remarkable C–H···S hydrogen bond between THT and TCNB is strengthened with increasing pressure[37] (Fig. 3). Moreover, from the steric hindrance point of view, the doping of THT into the lattice also increases the deformation of the neighboring molecules upon compression, inducing a larger deformation of perylene (Fig. S5†). The C–H···S hydrogen bond and the deformation of the perylene molecules could affect the distribution of their molecular orbitals. These factors should be related to the observed energy level change in the doped system. In addition, our calculation of the HOMO and LUMO of PTC-THT at ambient pressure shows that the HOMO is concentrated on the donor (perylene), while the LUMO is concentrated on the acceptor (TCNB) at ambient pressure (Fig. 4). Note that the HOMO energy level decreases while the LUMO energy level increases as pressure increases, leading to an increase

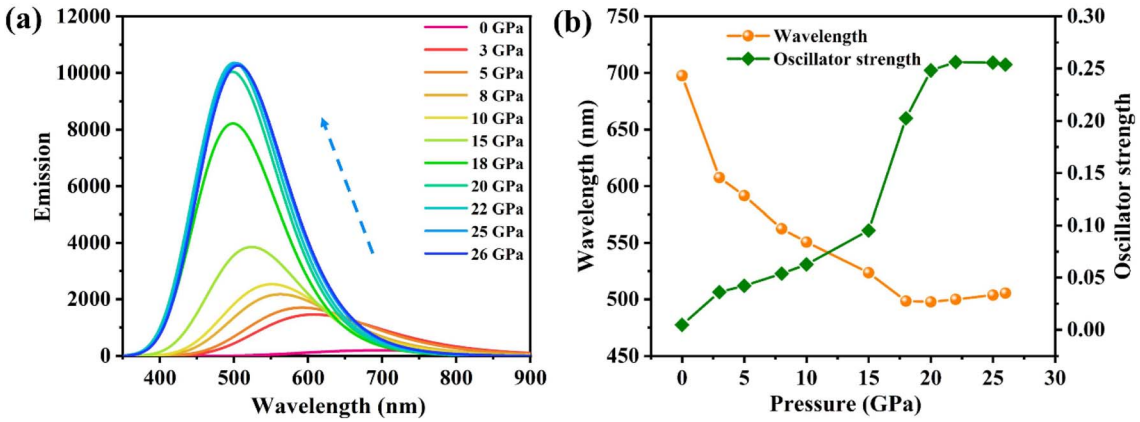

Fig. 2 The calculated (a) luminescence spectra, (b) emission wavelength and oscillator strength of PTC-THT at high pressures.

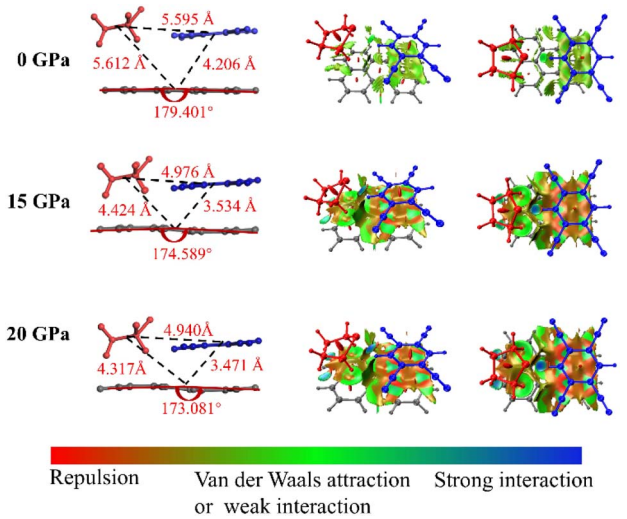

Fig. 3 The molecular structure and intermolecular interactions of PTC-THT at ambient pressure, 15 GPa and 20 GPa, respectively.

of the HOMO–LUMO energy gap and thus a blue shift of the emission wavelength.

Concerning the novel enhancement of the photoluminescence intensity, besides the effect of the intermolecular interactions and the change in the molecular configuration discussed above, the charge transfer in the doped cocrystal system should also contribute. As shown in Fig. 5, our Bader charge analysis shows that the number of electrons supplied by the donor group and received by the acceptor group increases gradually as the pressure increases, while the THT dopant also acts as an electron provider in the doped cocrystal. It is well known that the transition from the LUMO (TCNB) to the HOMO (perylene) is the basis for the luminescence process in the cocrystal, and the increase of the transition process indicates that there is a higher radiative transition process, resulting in a higher luminescence efficiency. Thus, the transition process between the LUMO and HOMO of PTC-THT increases due to the increased number of electrons provided by THT and TCNB, resulting in a higher luminescence efficiency, which well explains our experimental observations.

This strategy to design piezo-activated luminescent materials based on PTC cocrystals has been further examined by selecting several similar dopants with different charge transfer abilities, such as tetrahydropyrrole (THP) and tetrahydrofuran (THF). The luminescence spectra (Fig. S6†) of PTC doped with these two molecules (*i.e.*, PTC-THP and PTC-THF) also show similar anomalous piezo-activated luminescence behaviors. The difference is that, the enhancement effect and the range of emission wavelength blue shift are less pronounced for PTC-THP and PTC-THF than for PTC-THT. These differences could be well explained by the different modulations of these dopants brought to the PTC cocrystals. The three dopants all have the effect to force the TCNB to move to the edge of the perylene molecules as pressure increases, which affects the intermolecular interactions and molecular deformation, and thus the piezochromic luminescence behaviors. For example, the largest deformation of perylene appears in PTC-THT (Fig. S7†), which shows the most remarkable piezochromic luminescence response. What's more, the charge transfer ability of the dopants also has a close relation with the piezochromic luminescence intensity control of the corresponding doped cocrystals. Because the electronegativity of O is greater than that of N and S (O, N and S radicals on THT, THP and THF molecules, respectively), the order of electron donor ability is THT > THP > THF. As shown in Fig. S8,† our Bader charge calculation shows that the number of electrons gained by TCNB is relatively large in the range of 0 to 5 GPa for PTC-THF, gradually becoming much smaller. Meanwhile, the electron gain in the PTC-THP system can remain below 10 GPa. The different charge transfers from the dopant molecules will affect the gain and loss of electrons in the HOMO and LUMO of the corresponding cocrystals, and thus modulate their luminescence properties accordingly. The different electron donation abilities of the three dopants give piezochromic luminescence intensity enhancements in the order THT > THP >

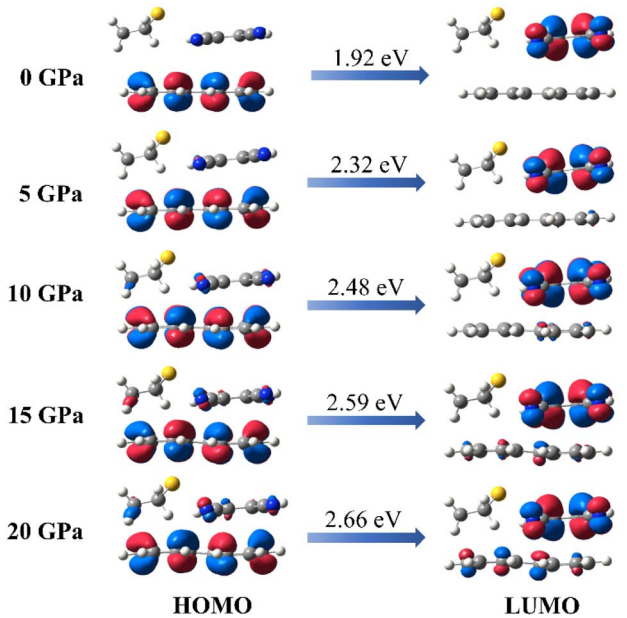

Fig. 4 The HOMO and LUMO of PTC-THT at high pressures.

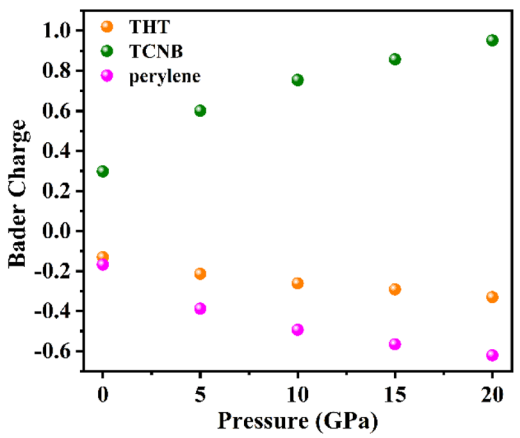

Fig. 5 The calculated Bader charge of PTC-THT at different pressures.

THF. Therefore, doping charge transfer molecules into cocrystals could be a universal and efficient strategy to design materials with desirable piezochromic luminescence properties for practical applications.

Experimental and computational details

Experimental details

Perylene (98%), 1,2,4,5-tetracyanobenzene (TCNB, 97%) and tetrahydrothiophene (THT, >99.0%) were purchased from Tokyo Chemical Industry Co., Ltd (TCI). All of the chemicals were used as received without further purification. The PTCs were obtained by a solvent evaporation method. Identical volumes (10 mL) of a 20 mM saturated solution of perylene and a 20 mM cor solution (solvent: THT) were mixed and the mixed solution was ultrasonicated for 15 minutes until a yellow solution was obtained. The blackish-green PTCs were obtained after evaporation of solvent from the solution after 7 days under ambient conditions. The as-synthesized PTCs had the same structure as those grown from CH_2Cl_2 (ref. 38) and tetrahydrofuran (THF);[27] the Cambridge Crystallographic Data Centre (CCDC) number is 1248027. The PTCs:THT were obtained by immersing PTCs in THT solvent sealed in a diamond anvil cell (DAC). In brief, PTCs were loaded into a 120 μm diameter hole drilled in a T301 stainless steel gasket, two drops of THT liquid were added and the DAC was quickly packaged after waiting for 10 s. High-pressure experiments were performed in the DAC. Pressure was calibrated by the fluorescence emission of ruby in the sample chamber. Scanning electron microscope (SEM) measurements were performed *via* a Hitachi Regulus 8100 field emission microscope equipped with an EDS spectrometer. Luminescence measurements were performed on a Raman spectrometer (Renishaw inVia) in the fluorescence mode with a 514.5 nm laser excitation. *In situ* high-pressure X-ray diffraction experiments were performed at the Rigaku Synergy Custom FR-X ($\lambda = 0.7093$ Å). Near ambient pressure X-ray diffraction experiments were performed at the Shanghai Synchrotron Radiation Facility, Beijing Synchrotron Radiation Facility ($\lambda = 0.6199$ Å) and Rigaku Japan R-AXIS-RAPID II ($\lambda = 1.5406$ Å).

Computational details

We used the Vienna *ab initio* simulation software package (VASP) to perform simulations using first-principles plane-wave pseudopotential density functional theory (DFT) to obtain the structure of PTC-THT at different hydrostatic pressures. The Perdew–Burke–Ernzerhof (PBE) generalized gradient approximation (GGA) was applied in the calculation. The quantum mechanics and molecular mechanics (QM/MM) method[34,35] with a two-layer ONIOM approach was built to investigate the properties of PTC-THT at high pressure. In the QM region, the central molecule (PTC-THT) was selected as the high layer and calculated with the QM method, while other surrounding molecules were treated as the low layer with the MM method in the MM region. M06-2X/6-31G(d,p) was selected to study the QM molecules and the universal force field (UFF) was used for MM, and electronic embedding was adopted to describe the coupling of the QM/MM interfaces. In the QM/MM geometric optimization process of the excited state, the molecules of the MM region are frozen, and only those of the QM region is free.[39–41] The intermolecular interactions in the cocrystals were studied by adopting the reduced density gradient (RDG) method within the Multiwfn software.[42] All the calculations above were carried out-in the Gaussian 09 package.[43]

Conclusions

A new strategy has been proposed to design luminescent materials with novel piezo-activated responses by molecular doping. The doping of THT into the luminescent perylene-TCNB cocrystal leads to the formation of a new weak but pressure-enhanced emission center, besides the strong emission band from the host cocrystals. This weak emission center shows a blue shift and giant luminescence enhancement upon compression, in contrast to the initial red shift and emission quenching of the host component. This results in a novel piezo-activated luminescence behavior with wide range emission wavelength modulation and giant intensity enhancement in the designed material. Further calculations show that such luminescence responses are related to the modulations of intermolecular interactions and electronic structure, as well as to enhanced charge transfer between the donor and acceptor in the cocrystals due to the strong electron donating ability of the THT dopant upon compression. This strategy can also be applied to other similar dopants to design and control piezoluminescence in materials, providing a new approach for designing novel materials with piezochromic luminescence.

Data availability

Essential data are provided in the main text and the ESI.† Data can be available from the corresponding author upon reasonable request.

Author contributions

M. Y. supervised the project. M. Y. and X. Y. conceived the study. X. Y. and Z. Y. carried out the theoretical study. C. Z. and T. X. designed and performed the experiments. L. Y. carried out the structure analysis. S. H., Q. L., R. L., and B. L. participated in the scientific discussions. M. Y., X. Y., and B. S. wrote and revised the manuscript.

Conflicts of interest

There are no conflicts to declare.

Acknowledgements

This work was supported financially by the National Natural Science Foundation of China (52225203) and National Key Research and Development Program of China (2018YFA0305900). We thank the Shanghai Synchrotron Radiation Facility and Beijing Synchrotron Radiation Facility for the XRD measurements. We also thank the Instrument and equipment sharing platform,

college of physics Jilin University for the SEM and part of XRD measurements.

Notes and references

1 Y. Sagara, S. Yamane, M. Mitani, C. Weder and T. Kato, *Adv. Mater.*, 2016, **28**, 1073–1095.
2 D. Yan, H. Yang, Q. Meng, H. Lin and M. Wei, *Adv. Funct. Mater.*, 2013, **24**, 587–594.
3 Y. Sagara, S. Yamane, T. Mutai, K. Araki and T. Kato, *Adv. Funct. Mater.*, 2009, **19**, 1869–1875.
4 Y. Liu, Q. Zeng, B. Zou, Y. Liu, B. Xu and W. Tian, *Angew. Chem., Int. Ed. Engl.*, 2018, **57**, 15670–15674.
5 Y. Sagara and T. Kato, *Angew. Chem.*, 2008, **120**, 5253–5256.
6 H. Sun, S. Liu, W. Lin, K. Y. Zhang, W. Lv, X. Huang, F. Huo, H. Yang, G. Jenkins, Q. Zhao and W. Huang, *Nat. Commun.*, 2014, **5**, 3601.
7 Z. Zong, Q. Zhang, S. H. Qiu, Q. Wang, C. Zhao, C. X. Zhao, H. Tian and D. H. Qu, *Angew. Chem., Int. Ed. Engl.*, 2022, **61**, e202116414.
8 J. Wang, J. Mei, R. Hu, J. Z. Sun, A. Qin and B. Z. Tang, *J. Am. Chem. Soc.*, 2012, **134**, 9956–9966.
9 X. Cheng, D. Li, Z. Zhang, H. Zhang and Y. Wang, *Org. Lett.*, 2014, **16**, 880–883.
10 S. Ishizaka, Y. Hinatsu, K. Tsuge, H. Ito, T. Saito, N. Oshima, M. Kato, N. Kitamura, M. Wakeshima and M. Sawamura, *J. Am. Chem. Soc.*, 2008, **130**, 10044–10045.
11 Y. Sagara, T. Mutai, I. Yoshikawa and K. Araki, *J. Am. Chem. Soc.*, 2007, **129**, 1520–1521.
12 Q. Lou, X. Yang, K. Liu, Z. Ding, J. Qin, Y. Li, C. Lv, Y. Shang, Y. Zhang, Z. Zhang, J. Zang, L. Dong and C.-X. Shan, *Nano Res.*, 2021, **15**, 2545–2551.
13 X. Lu, Y. Wang, C. C. Stoumpos, Q. Hu, X. Guo, H. Chen, L. Yang, J. S. Smith, W. Yang, Y. Zhao, H. Xu, M. G. Kanatzidis and Q. Jia, *Adv. Mater.*, 2016, **28**, 8663–8668.
14 X. Guo, N. Zhu, S. P. Wang, G. Li, F. Q. Bai, Y. Li, Y. Han, B. Zou, X. B. Chen, Z. Shi and S. Feng, *Angew. Chem., Int. Ed. Engl.*, 2020, **59**, 19716–19721.
15 Z. Q. Yao, J. Xu, B. Zou, Z. Hu, K. Wang, Y. J. Yuan, Y. P. Chen, R. Feng, J. B. Xiong, J. Hao and X. H. Bu, *Angew. Chem., Int. Ed. Engl.*, 2019, **58**, 5614–5618.
16 S. Guo, Y. Zhao, K. Bu, Y. Fu, H. Luo, M. Chen, M. P. Hautzinger, Y. Wang, S. Jin, W. Yang and X. Lu, *Angew. Chem., Int. Ed. Engl.*, 2020, **59**, 17533–17539.
17 J. Zou, Y. Fang, Y. Shen, Y. Xia, K. Wang, C. Zhang and Y. Zhang, *Angew. Chem., Int. Ed. Engl.*, 2022, **61**, e202207426.
18 M. Wu, H. Liu, H. Liu, T. Lu, S. Wang, G. Niu, L. Sui, F. Bai, B. Yang, K. Wang, X. Yang and B. Zou, *J. Phys. Chem. Lett.*, 2022, **13**, 2493–2499.
19 Y. Yan, N. Sun, F. Li, X. Jia, C. Wang and D. Chao, *ACS Appl. Mater. Interfaces*, 2017, **9**, 6497–6503.
20 J. Cui, M. Yao and Y. Hua, *Sci. Rep.*, 2015, 13398.
21 W. Jing, A. Li, S. Xu, B. Li, C. Song, Y. Geng, N. Chu, H. Jian and W. Xu, *J. Mater. Chem. C*, 2018, **6**, 8958–8965.
22 X. Zhao, M. Wu, H. Liu, Y. Wang, K. Wang, X. Yang and B. Zou, *Adv. Funct. Mater.*, 2021, **32**, 2109277.
23 C. Feng, K. Wang, Y. Xu, L. Liu, B. Zou and P. Lu, *Chem. Commun.*, 2016, **52**, 3836–3839.
24 K. Nagura, S. Saito, H. Yusa, H. Yamawaki, H. Fujihisa, H. Sato, Y. Shimoikeda and S. Yamaguchi, *J. Am. Chem. Soc.*, 2013, **135**, 10322–10325.
25 Y. Dong, B. Xu and J. Zhang, *Angew. Chem.*, 2012, **51**, 10782–10785.
26 H. Liu, Y. Gu, Y. Dai, K. Wang, S. Zhang, G. Chen, B. Zou and B. Yang, *J. Am. Chem. Soc.*, 2020, **142**, 1153–1158.
27 C. Zhai, X. Yin, S. Niu, M. Yao, S. Hu, J. Dong, Y. Shang, Z. Wang, Q. Li, B. Sundqvist and B. Liu, *Nat. Commun.*, 2021, **12**, 4084.
28 M. Baba, T. Katori, M. Kawabata, S. Kunishige and T. Yamanaka, *J. Phys. Chem. A*, 2013, **117**, 13524–13530.
29 Y. L. Lei, Y. Jin, D. Y. Zhou, W. Gu, X. B. Shi, L. S. Liao and S. T. Lee, *Adv. Mater.*, 2012, **24**, 5345–5351.
30 P. Wu, L. Zhou, Z. Zhen, S. Xia and L. Yu, *J. Photochem. Photobiol., A*, 2022, **426**, 113727.
31 J. Han, W. Feng, D. Y. Muleta, C. N. Bridgmohan, Y. Dang, G. Xie, H. Zhang, X. Zhou, W. Li, L. Wang, D. Liu, Y. Dang, T. Wang and W. Hu, *Adv. Funct. Mater.*, 2019, **29**, 1902503.
32 Y. Sun, Y. Lei, L. Liao and W. Hu, *Angew. Chem., Int. Ed. Engl.*, 2017, **56**, 10352–10356.
33 Y. Sun, Y. Lei, H. Dong, Y. Zhen and W. Hu, *J. Am. Chem. Soc.*, 2018, **140**, 6186–6189.
34 T. Zhang, W. Shi, D. Wang, S. Zhuo, Q. Peng and Z. Shuai, *J. Mater. Chem. C*, 2019, **7**, 1388–1398.
35 Y. Zeng, Y. Niu, Q. Peng and X. Zheng, *J. Phys. Chem. A*, 2022, **126**, 4147–4155.
36 S. Hu, Z. Yao, X. Ma, L. Yue, L. Chen, R. Liu, P. Wang, H. Li, S. T. Zhang, D. Yao, T. Cui, B. Zou and G. Zou, *J. Phys. Chem. Lett.*, 2022, **13**, 1290–1299.
37 S. K. Erin, R. Johnson, P. Mori-Sánchez, J. Contreras-García, A. W. Y. Aron and J. Cohen, *J. Am. Chem. Soc.*, 2010, **132**, 6498.
38 H. Bock, W. Seitz, M. Sievert, M. Kleine and J. W. Bats, *Angew. Chem., Int. Ed. Engl.*, 1996, **35**, 2244–2246.
39 J. Xue, Q. Liang, R. Wang, J. Hou, W. Li, Q. Peng, Z. Shuai and J. Qiao, *Adv. Mater.*, 2019, **31**, e1808242.
40 Y. Sun, H. Geng, Q. Peng and Z. Shuai, *ChemPhysChem*, 2020, **21**, 952–957.
41 H. Ma, H. Yu, Q. Peng, Z. An, D. Wang and Z. Shuai, *J. Phys. Chem. Lett.*, 2019, **10**, 6948–6954.
42 T. Lu and F. Chen, *J. Comput. Chem.*, 2012, **33**, 580–592.
43 M. J. T. Frisch, G. W. Trucks, H. B. Schlegel, G. E. Scuseria, M. A. C. Robb, J. R. Cheeseman, G. Scalmanim V. Barone, G. A. Petersson, and H. Nakatsuji, *Gaussian 09*, Wallingford CT, Gaussian, Inc., 2009.